Journal of Cleaner Production 322 (2021) 129105

Contents lists available at ScienceDirect

Journal of Cleaner Production

journal homepage: www.elsevier.com/locate/jclepro

Development of cement-free bio-based cold-bonded lightweight aggregates (BCBLWAs) using steel slag and miscanthus powder via CO_2 curing

Y.X. Chen [a,b], G. Liu [c,*], K. Schollbach [b], H.J.H. Brouwers [a,b]

[a] State Key Laboratory of Silicate Materials for Architectures, Wuhan University of Technology, Wuhan, 430070, China
[b] Department of the Built Environment, Eindhoven University of Technology, AP Eindhoven, 5612, the Netherlands
[c] School of Human Settlements and Civil Engineering, Xi'an Jiaotong University, Xi'an, China

ARTICLE INFO

Handling editor: Zhen Leng

Keywords:
Miscanthus powders
Converter steel slag
CO_2 curing
Cold-bonded lightweight aggregate
Concrete

ABSTRACT

Bio-based lightweight aggregates are a novel type of lightweight aggregates. The use of plant-based aggregates in concrete effectively decreases its bulk density, the environmental impact and improve the thermal insulation property. However, the application of plant-based aggregate in ordinary cement-based concrete still faces critical problems, for instance, the polysaccharide leached from the plant retards the hydration of clinker and lead to degradation of concrete strength. In this study, a novel bio-based cold-bonded lightweight aggregates (BCBLWAs) was developed with the use of converter steel slag and miscanthus powder via CO_2 curing. The aggregates using steel slag as a binder show relatively high strength and low density with the use of miscanthus. The polysaccharide leached from miscanthus powder, which negatively influences the cement-based aggregates, has no influence on the artificial carbonated steel slag aggregate. The developed BCBLWAs obtained compressive strengths from 0.58 MPa to 5.3 MPa and loose bulk densities from 550 kg/m^3 to 1300 kg/m^3. The reaction products and microstructure of BCBLWAs after carbonation curing were characterized by TGA, XRD, SEM and nitrogen physisorption. The CO_2 uptake capacity of BCBLWAs was also evaluated. Furthermore, the prepared BCBLWAs were utilized to prepare a lightweight concrete, which obtained optimal compressive strength (28.5 MPa), dry bulk density (1630 kg/m^3) and thermal insulation (0.439 W/(m·K)). The effect of BCBLWAs on the hydration of cement was also evaluated to be minor and only showed a slight retardation effect. The lowest thermal insulation of BCBLWAs incorporated lightweight concrete reached 0.255 W/(m·K).

Credit author statement

Y.X. Chen: Conceptualization; Methodology; Investigation; Data curation; Formal analysis; Validation; Writing – original draft. G.Liu: Writing – Conceptualization; Methodology; Investigation; Data curation; Formal analysis; Validation; Writing – review & editing. K. Schollbach: Supervision; Writing – review & editing, H.J.H. Brouwers: Supervision; Writing – review & editing; Project administration.

1. Introduction

Lightweight concrete is widely used in construction and buildings. It can effectively reduce the mass and show superior thermal insulation and sound absorption properties, while maintaining adequate strength (Chandra and Berntsson, 2002). The combination of cementitious materials and different lightweight aggregates (LWAs) can be utilized to produce various kinds of lightweight aggregate concretes, for instance, ultralightweight concrete incorporated with expanded glass or expanded polystyrene foam (Kan and Demirboga, 2009; Spiesz et al., 2013; Ducman and Mladenovic, 2002; Yu et al., 2013). The properties of LWA, such as density, strength and thermal conductivity, are the key factors influence the performance of lightweight concrete. Furthermore, the LWA accounts for the main cost and energy consumption of lightweight concrete.

Generally, the sintering process contributes to a high CO_2 emission of commercial LWAs production, which is indispensable to produce the porous structure of aggregates. For example, expanded glass derived lightweight aggregate, where the raw glass is crushed, ground and mixed with blowing agents before granulation. After that the formed granules are heated in a rotary kiln to more than 1400 °C (Ducman and Mladenovic, 2002). This mechanism of high temperatures to produce porous structure is also applied to lightweight expanded clay aggregate

* Corresponding author. School of Human Settlements and Civil Engineering, Xi'an Jiaotong University, Xi'an, China.
E-mail addresses: gang0721@outlook.com, gang.liu@xjtu.edu.cn (G. Liu).

https://doi.org/10.1016/j.jclepro.2021.129105
Received 27 April 2021; Received in revised form 26 August 2021; Accepted 18 September 2021
Available online 19 September 2021

(LECA) and perlite. The LECA is heated to around 1200 °C in a rotary kiln to yield gases, expand the clay and produce a honeycomb structure (Hammer et al., 2000). Perlite needs to be heated to 760–1100 °C, and the moisture is converted to gas and resulting in a lightweight high porosity material (PAPADOPOULOS et al., 2008). Therefore, a lowered embedded energy of lightweight aggregate is in dire needed.

Recently, more studies have focused on the production of economic LWAs, using the cold-bonding process to produce sustainable lightweight aggregates by various industrial by-products (Tang et al., 2020b; Tang and Brouwers, 2017, 2018). Normally, ordinary Portland cement (OPC) is a necessary binder during the pelletizing process to provide adequate strength of cold-bonded LWAs (CBLWAs), which plays as an adhesive agent. For instance, cement slurry and fine incineration bottom ash were used to produce lightweight aggregates that show strengths from 0.3 to 2.0 MPa (Tang et al., 2019). In another study, the application of 10–15% of CEM I 42.5 N cement in CBLWA provides a compressive strength of 5.7 MPa after 28 days normal curing (Tang and Brouwers, 2017). Table 1 shows the summary of the studies using CBLAs in lightweight concrete. Using this method, the artificial lightweight aggregates produced at room temperatures, while still showing considerable strength (Tang et al, 2017, 2020a, 2020b, 2020b).

However, Portland cement accounts for a high amount of CO_2 emission. Therefore, alternative binder system like geopolymer or alkali-activated materials are also utilized in cold-bonded lightweight aggregates. For instance, GGBS and FA utilized as binders have been investigated (Baykal and Döven, 2000; Di Palma et al., 2015; Geetha and Ramamurthy, 2010b; Ramamurthy and Harikrishnan, 2006). Alkaline activator, including Na_2SiO_3 and NaOH, have been incorporated in the production of geopolymer CBLAs (Bui et al., 2012; Geetha and Ramamurthy, 2013). However, FA and GGBS are not regarded as solid waste in recent years and become more valuable in concrete production. Hence, it is interesting to find a solid waste to be utilized as a binder to produce CBLWAs. To the authors' knowledge, industrial by-product such as converter steel slag has never been reported to be used as a binder in the production of CBLAs.

Converter steel slag is a by-product of the steel making process (Wang, 2016). In the European Union, there is more than 100 million tons of steel slag currently landfilled and will continue to produce millions of tons of steel slag every year (EUROFER, 2019). The main crystalline phases in CSS are larnite, wüstite, brownmillerite, free lime and magnetite (Reddy et al., 2019). Although C_2S can provide some hydraulic properties of CSS, the large amount of other inert phases and the presence of free lime make it difficult to use as a binder or aggregate in concrete (Belhadj et al., 2012; Wang and Yan, 2010). However, carbonation of steel slag can transform C_2S and free lime to calcite and solve the volumetric instability issue. The main carbonation reaction happens as follows:

$$Ca_2SiO_4 + CO_2 + H_2O \rightarrow CaCO_3 + SiO_2 + H_2O \quad (1)$$

$$CaO + CO_2 + H_2O \rightarrow CaCO_3 + H_2O \quad (2)$$

The C_2S and free lime react with CO_2 and in presence of water, forming calcite and amorphous silica. In this process, the carbonation products can bond particles together and contribute to the development of the strength, for example, carbonated steel slag mortars (Liu et al., 2020a,b). Therefore, the carbonation process of converter steel slag is predicted to replace the hydrated cement as an adhesive agent in the production of CBLWAs. However, the density of converter steel slag is very high (around 3.9 kg/m^3), which makes it difficult to be applied in the manufacture of lightweight aggregate (Ferreira et al., 2016). Furthermore, the thermal conductivity of steel slag is relatively high, reaching 0.85–1.2 W/(m·K) or even higher (Barra et al., 2016). The insulation property is closely related to the density of the materials. Therefore, finding a sustainable and renewable lightweight additive for the sake of reducing the density of carbonated steel slag, and further to prepare novel lightweight aggregate is very important.

On the other hand, biomaterials are recently investigated as interesting substitution of fossil fuel materials like polymers, which can be applied in construction materials (Q. Liu et al., 2020; Liu et al., 2019). Natural fibers is an ultralow density and high porosity biomaterial and can be used as a kind of LWA in lightweight concrete, for instance, jute, hemp and miscanthus (Bheel et al., 2021). Among these biomaterials, the incorporation of miscanthus fibers in LWA production can effectively reduce the density, while contributing to the improvement of thermal insulation and acoustic absorption (Chen et al., 2017, 2020). Miscanthus shows two major advantages as compared to common renewable materials like conifers. These are the thermal insulating qualities and in addition the very high firmness of the plant material (Moll et al., 2020). A cross-section of the miscanthus shoot shows, that there is the parenchyma which provides the thermal insulation and around the parenchyma there are three rings with relevance to firmness: the epidermis, the thick sclerenchyma characteristics and the radial allocation of vascular bundles with its own firmness texture (Pude et al., 2004). However, miscanthus powders have very high water absorption and are difficult to be used in concrete directly. This is due to the high surface area of miscanthus powder. Preliminary results also showed that miscanthus powders severely delay clinker hydration which makes it difficult to form cement-based pellets (Chen et al., 2017; Fan et al., 2012). In summary, combining miscanthus powder and converter steel slag for LWA production by using carbonation curing could solve above incompatibilities, such as retardation effect and high density and thermal conductivity issue. In this way, the LWA could be produced without cement. This makes it possible to produce sustainable LWA that are not affected by the polysaccharide leached from natural fibers and also significantly reduce the density and thermal conductivity of steel slag pellets. It is also expected that the moderate amount of miscanthus powder (MP) in aggregates could accelerate the carbonation of steel slag, resulting in a higher strength of the CBLAs, thanks to the high porosity and water retention of MP.

In this study, lightweight aggregates are produced by the carbonation of cold-bonded steel slag and miscanthus powder. The miscanthus plays a role as lightweight biofibres and accelerates the carbonation reaction. The microstructure and carbonation products of the produced bio-based cold-bonded lightweight aggregates (BCBLWAs) are

Table 1
CBLAs in recent studies, showing most of the CBLAs components contain cement.

Components	Curing method	LBD (kg/m^3)	WAB (wt-%)	WC (wt-%)	BS (MPa)	Literatures
Cement, class-F FA	RH 70% at 20 °C	1460	21.15	22	–	Güneyisi et al. (2015)
Waste concrete powder, cement, slag, $Ca(OH)_2$	CO_2 curing; RH 60%	926–972	9.30–36.30	–	0.75–2.98	Jiang et al. (2020)
Cement, Class-F FA, EPP	RH 65%–99%	510–650	30–52	–	0.20–3.55	Tajra et al. (2018)
Cement, lime, class-F FA, $Ca(OH)_2$, Na_2SO_4	In water	750–980	19–23	30–33	–	Geetha and Ramamurthy (2010a)
Class-F FA, GGBS, CEM I 42.5	RH 70% at 21 °C		4–20	18–20	–	Gesoğlu et al. (2012)
Class-F FA, quarry dust, cement	In water	950–1100	16–21	–	6.15–8.32	Thomas and Harilal (2015)
MSWI FA, CEM II 42.5 R, lime, coal fly ash	Seal curing	980	14.9	–	7.5	Tang et al. (2017)

*LBD: loose bulk density; WAB: water absorption; WC: water content; BS: bulk crushing strength; FA: fly ash; EPP: expanded perlite powder; MSWI FA: municipal solid waste incineration fly ash; GGBS: granulated ground blast slag.

characterized by SEM, TGA, XRD and nitrogen physisorption. The CO_2 uptake capacity of BCBLWAs is also calculated. The mechanical properties of BCBLWAs are measured by individual pellet strength and bulk crushing resistance. Moreover, a lightweight concrete with the incorporation of BCBLWAs is prepared. The developed novel lightweight concrete is characterized by dry density, compressive strength, and thermal insulation properties. The result of this study shows promising application of steel slag and miscanthus powder as the raw materials in the production of sustainable and negative CO_2 footprint CBLAs.

2. Experiments and methodology

2.1. Raw materials

Converter steel slag was provided by Tata steel, IJmuiden, the Netherlands (specific density is 3.9 kg/m^3). Miscanthus powder (below 1 mm) was provided by Vibers, the Netherlands. These two materials are the ingredients to prepare BCBLWAs.

Ordinary Portland cement (CEM I 52.5 R) was used to prepare BCBLWAs lightweight aggregate concrete, which was provided by ENCI. The oxide composition of steel slag and CEM I 52.5 R are shown in Table 2. The mineral composition was determined using X-ray diffraction (XRD) analysis, which is shown in Fig. 1 (a). The converter steel slag mainly consists of brownmillerite, C_2S, wüstite and magnetite. Minor amounts of free lime and C_3S are also possible. The MgO mainly exists in the mineral phase of wuestite, which is a solid solution between MgO and FeO. The content of free lime in the converter slag from Tata Steel is very low (<2%). The particle size distribution of finely grounded steel slag using a disc mill is presented in Fig. 1 (b). The specific surface area of steel slag and cement is 0.42 m^2/g and 1.00 m^2/g, respectively, tested by nitrogen physisorption using BET theory. The specific density of steel slag and cement is 3.9 g/m^3 and 3.15 g/m^3, respectively.

The monomeric polysaccharides' concentration of miscanthus powder was tested by using High-Performance Anion-Exchange Chromatography (HPAEC) after H_2SO_4 hydrolysis in mg/ml were: For example, Arabinose 0.06, Galactose 0.09, Glucose 0.19, Xylose 0.16 and Mannose 0.05 as shown in Table 3. The component of miscanthus are mainly cellulose, hemicellulose and lignin, which account for 40.21%, 43.24% and 17.93% of the total mass, respectively (Chen et al., 2017). The SEM images of the miscanthus powders (Fig. 2) show a porous structure with pore sizes of around tens of micrometres. The particle shape of miscanthus powder is quite heterogeneous, with particle size ranging from 50 μm to 1 mm. The water absorption of MP is quite high according to previous research, showing a water absorption capability of above 300% (Chen et al., 2017). The density of the MP is around 300 kg/m^3, which is quite low compared to converter steel slag.

2.2. Pelletizing procedure

Fig. 3 shows the pelletizing process of BCBLWAs manufactured with miscanthus powders and steel slag. The disc pelletizer was used to produce the artificial aggregates. The model was D-7736, Maschinenfabrik Gustav Eirich, Germany. The size of the pelletizer was 40 cm in diameter and 10 cm in collar height. The speed and angle were adjusted to give an optimal production efficiency. Herein, production efficiency was assessed as the ratio between the mass of pellets produced obtaining a size of more than 4 mm and the total mass of the raw steel slag and miscanthus used in the pelletization process. The optimal vertical angle of the pan was determined to be 75° and the rotating speed was 60 rpm during the production. It can be seen from Table 4 that the production efficiency was increased by increasing the steel slag content, reaching the highest value of 96% when no MP was used. This increase in production efficiency can be attributed to the role of steel slag as a binder, because that sticks together forming pellets, contributing to hold the MP particles together due to being much stickier. The starting mixtures of steel slag and miscanthus powders used for BCBLWAs were first mixed via a planetary mixer. Then around 500 g of the mixed powders were placed on the rotating pan. After about 3 min rotating, around 50 g of distilled water was sprayed slowly onto the mixed powder in the pan using a spray bottle in 10 min. After small balls formed in the pan, the pan continued running for 5 min to make the aggregate grow. Afterwards, the first round as-prepared aggregate would drop off simultaneously from the bottom of the pan. The next batch was prepared with the addition of another 500 g of dry mixed powder and followed the same procedure again. The freshly prepared BCBLWAs were placed in a sealed plastic box for further CO_2 curing.

For the CO_2 curing process, the BCBLWAs were placed in a CO_2 chamber and carbonated for 3 days to complete the carbonation process. The CO_2 concentration and the humidity were set at 20% and 75%, respectively. The temperature during curing was constant, around 20 °C. The pressure used is atmospheric pressure, i.e. 101.3 kPa.

In order to determine the optimal volume ratio of steel slag and miscanthus powders, 5 batches of artificial aggregates were pelletized (SS:MP = 100:0, 90:10, 80:20, 65:35 and 50:50 in volume percent). The recipe for BCBLWAs in this study is shown in Table 4.

2.3. Lightweight concrete (LWC) preparation

The mix design for LWC-BCBLWAs is shown in Table 5. The preparation of lightweight concrete with the incorporation of BCBLWAs is described as follows: (1) CEM I 52.5 R was dry mixed in the planetary mixer for 1 min (2) Tap water was added into the mixer with a w/b ratio of 0.5 and continued mixing for 3 min (3) The as-prepared BCBLWAs was added into the cement paste and continued mixing for 5 min (4) After the fresh grout was homogeneous, the fresh grout was poured into the mould without compaction. The grout showed self-compacting property due to the spherical shape of BCBLWAs. (5) The mould was sealed with plastic film for 1 day and demoulded the next day. Seal curing was applied to cure the samples until the age of 7 and 28 days.

2.4. Characterization methods

2.4.1. Physical and mechanical properties of BCBLWAs

The loose bulk density test was carried out according to EN 1097–3 (EN1097-3, 1998). The water absorption test was carried out according to EN 1097–6 (EN1097-6, 2005). The particle size of the tested pellets was around 4–8 mm. The water content of BCBLWAs was determined by heating the pellets in the oven at 110 °C for 24 h and then measuring the remaining mass of the pellets. Hence, the water content was the weight difference before and after heating divided by the original mass of the pellets. The mechanical property of the individual pellet of BCBLWAs with different sizes were tested in an MTS Criterion equipped with a load cell of 5000 N at a speed of 0.6 mm/min until collapse. The maximum force was used to calculate the individual crushing strength according to Eq. (1) (Baykal and Döven, 2000). Around 20 pellets were used as representatives for every batch of BCBLWAs prepared.

Table 2
The oxides composition of raw materials used.

Materials (wt%)	CaO	SiO_2	Al_2O_3	Fe_2O_3	TiO_2	P_2O_5	MgO	MnO	V_2O_5	SO_3	LOI
Steel slag	41.55	11.47	2.24	31.35	1.56	1.30	3.78	4.78	1.14	–	0.72
Cement	64.64	20.08	4.98	3.24	0.30	0.42	1.98	0.10	–	3.13	0.51

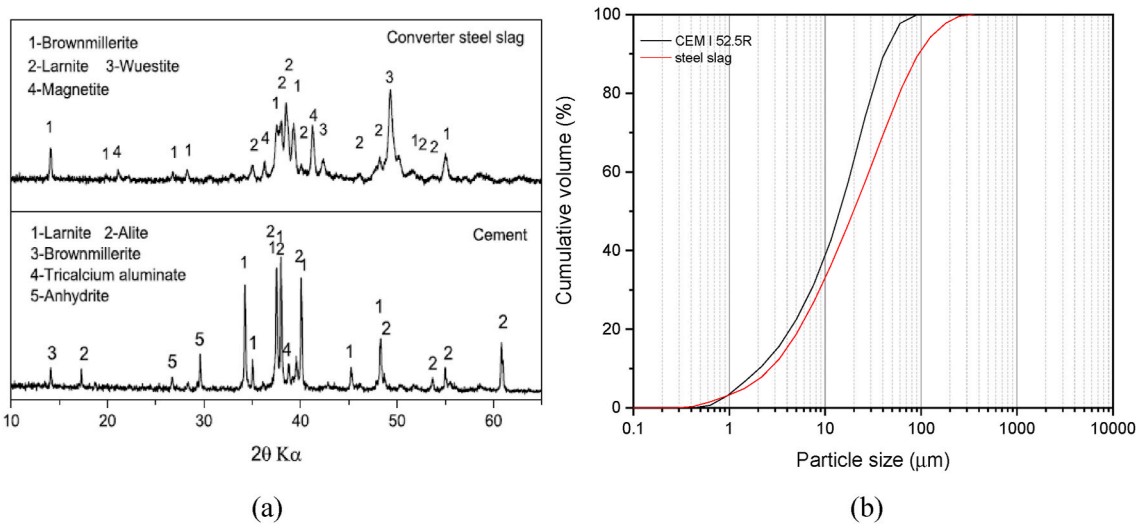

Fig. 1. XRD (a) and PSD (b) of the used converter steel slag and cement.

Table 3
The components from the leachate of miscanthus.

Miscanthus Analysis: Components from the leachate	Concentration (mg/ml)
Glucuronic acid	0.01
Galacturonic acid	0.02
Arabinose	0.06
Galactose	0.09
Glucose	0.19
Xylose	0.16
Mannose	0.05

$$\sigma = \frac{2.8P}{\pi d^2} \tag{3}$$

where σ (MPa) is the crushing strength of each pellets tested, P (N) is the maximum force each pellet can withstand, d (mm) is the approximate diameter of the round pellet produced.

The bulk crushing resistance (CR) of the BCBLWAs aggregates was measured according to EN 13055–1 (Annex Procedure 1) (EN13055-1, 2002). The proper amount of sample pellets was filled in the cylinder and then compressed to a height of 20 mm. The following equation was used to calculate the CR:

$$C = \frac{L+F}{A} \tag{4}$$

where C is the crushing resistance of (MPa), L is the force generated by the load cell (N), F is the compression force (N), and A is the compressed area (mm^2), equals to $\pi d^2/4$.

2.4.2. Reaction products and microstructure analysis of BCBLWAs

The microstructure of the BCBLWAs was observed with scanning electron microscopy (SEM), by using a JOEL JSM-5600 instrument at an accelerating voltage of 15 kV. The specific surface area and pore size distribution of BCBLWAs were measured after grinding and sieving using a 68 μm sieve to remove most of the miscanthus powder. Therefore, the surface area is not influenced by the miscanthus powder, which is believed to be removed out by the sieving process. Finally, it was measured by nitrogen physisorption using a Micromeritics Tristar 2000 with BET and BJH method, respectively. The CO_2 uptake capacity of the BCBLWAs was measured by using thermogravimetric analysis (TGA) with a NETZSCH STA449-F1 instrument at a heating rate of 10 °C/min under nitrogen atmosphere. The quantification of the CO_2 uptake per gram BCBLWAs was determined by the mass loss from 600 to 800 °C, which is the temperature where decomposition of calcite takes place. The following equation was used to calculate the CO_2 uptake capability of BCBLWAs per unit (Liu et al., 2020a, 2020b).

$$CO_2(uptake) = \frac{M_{600} - M_{800}}{M_{800} + M_{fiber}} \times 100\% \tag{5}$$

The crystalline phases of carbonated BCBLWAs were detected by X-ray diffraction analysis. The parameters chosen were as follows: Co tube, 40 KV, 30 mA, 0.02°/step, 0.2°/min, with variable divergence slits V20. The BCBLWAs samples were first ground and passed through a 68 μm

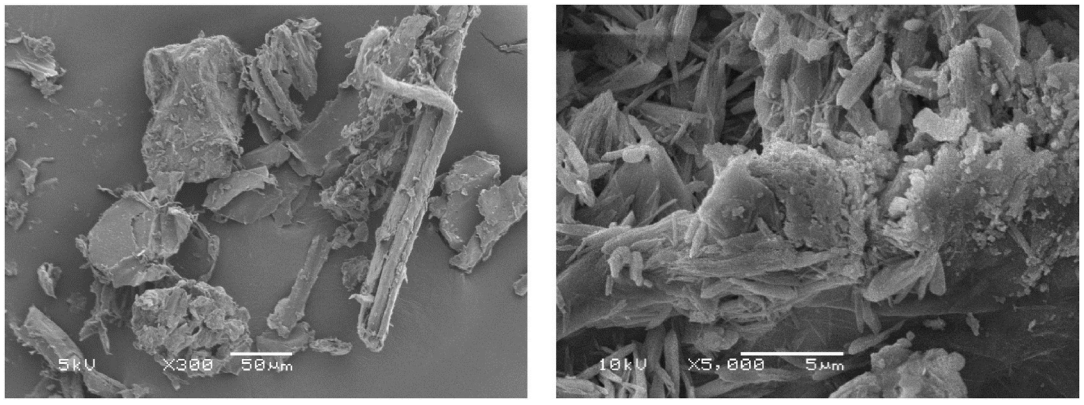

Fig. 2. SEM images of the used miscanthus powder (a) magnification × 300 (b) magnification × 5000.

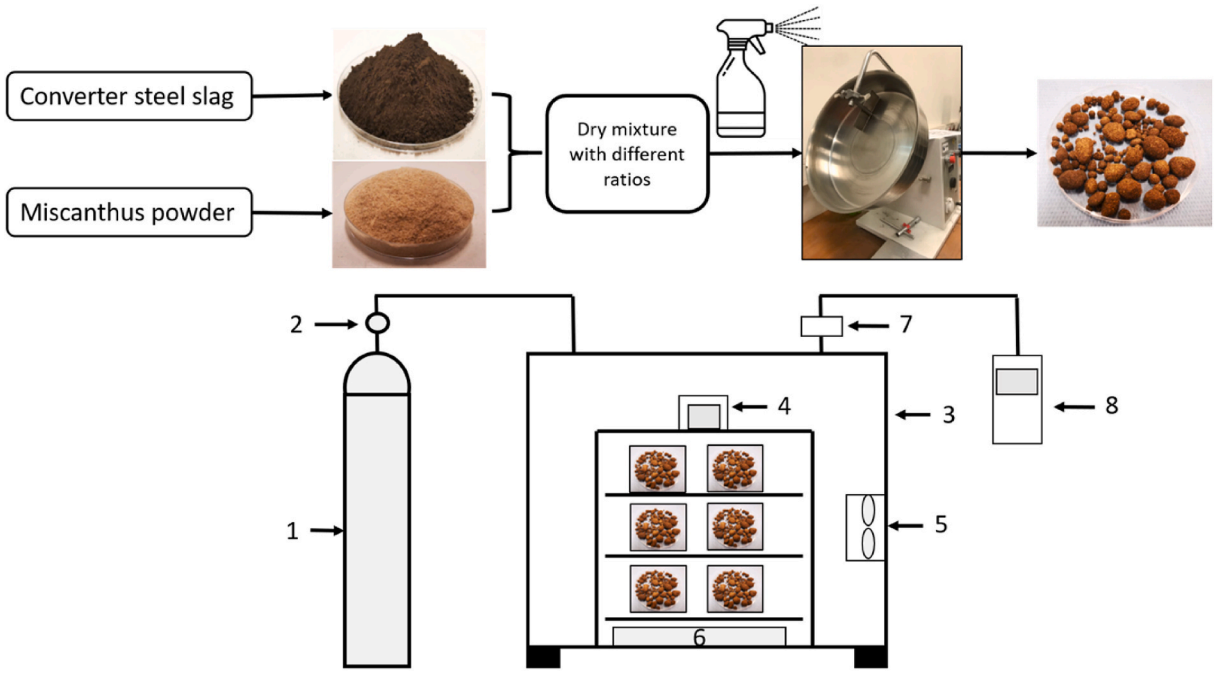

Fig. 3. Schematic process of the production of BCBLWAs with steel slag and miscanthus powder. (1. CO_2 2. Regulator 3. Carbonation chamber 4. Humidity and temperature meter 5. Fan 6. NaCl solution 7. CO_2 probe 8. CO_2 meter).

Table 4
Recipe for BCBLWAs with different volume ratio of steel slag and miscanthus powder.

Groups Materials	SS100	SS90MP10	SS80MP20	SS65MP35	SS50MP50
Steel slag (g/vol%)	1000/(100%)	960/(90%)	919/(80%)	838/(65%)	735/(50%)
Miscanthus powder (g/vol%)	0/0	41/(10%)	82/(20%)	162/(35%)	264/(50%)
Production efficiency (%)	96.5	88.2	80.3	73.6	65.9

Table 5
The mix design of lightweight concrete incorporated with 50 vol% BCBLWAs (kg/m^3).

Groups	CEM I 52.5 R (kg/m^3)	Water (kg/m^3)	BCBLWAs (kg/m^3)	BCBLWAs (vol%)
LWC-SS100	608	304	1400	50
LWC-SS90MP10	608	304	1050	50
LWC-SS80MP20	608	304	900	50
LWC-SS65MP35	608	304	750	50
LWC-SS50MP50	608	304	500	50

sieve to remove most of the miscanthus powders. The remaining material was used to prepare the XRD samples.

2.4.3. Characterization of LWC-BCBLWAs

The fresh density of LWC incorporated with BCBLWAs was measured following EN 12350–6 (2009). After mixing, the LWC-BCBLWAs was cast into moulds of 100 mm × 100 mm × 100 mm and 40 mm × 40 mm × 160 mm. The samples were demoulded after 1 d and the dry density was determined following EN 12390–7 (2009). The compressive and flexural strength of the LWC-BCBLWAs were tested at the age of 7 and 28 days. After 28 days curing, the LWC-BCBLWAs cubes were first dried at 105 °C overnight to a constant mass. The heat transfer analyser ISOMET model 2104 was used to determine the thermal conductivity of the LWC-BCBLWAs. The isothermal calorimeter (TAM Air, Thermometric) with three channels was used to test the influence of BCBLWAs on the hydration of Portland cement CEM 52.5 R using calorimeter pots with a volume of 100 ml. The volumetric ratio of BCBLWAs to the volume of cement paste was 1:1. All measurements were conducted for 72 h under a constant temperature of 20 °C. The heat release and heat flow results were normalized by mass of binder, miscanthus and de-ionized water.

3. Results and discussions

3.1. Physical properties of the produced BCBLWAs

The water content and water absorption of the prepared BCBLWAs are shown in Table 6. The water content of BCBLWAs is influenced by the percentage of miscanthus powder in the LWA mix because the miscanthus powder has a much larger intra-particle porosity than the carbonated steel slag, thus absorbs more water during pelletization. As indicated in (Chen et al., 2017), the intra-particle porosity of MP is around 77%, As seen from Table 6, the water content of BCBLWAs

Table 6
Water content, water absorption and densities of BCBLWAs.

Groups	SS100	SS90MF10	SS80MF20	SS65MF35	SS50MF50
Water content (%)	1.14 ± 0.1	2.98 ± 0.2	4.20 ± 0.3	6.80 ± 0.2	18.1 ± 0.9
Water absorption (%)	5.86 ± 0.2	5.09 ± 0.1	7.77 ± 0.2	18.83 ± 0.5	41.06 ± 1.2
Loose bulk density (kg/m^3)	1630 ± 12	1300 ± 10	1050 ± 11	760 ± 9	550 ± 7
Particle density (kg/m^3)	2800 ± 26	2130 ± 15	1760 ± 19	1390 ± 20	1080 ± 32

increases with the increasing content of MP from 1.14% to 18.1%. However, according to literatures, many cold-bonded lightweight aggregates have a water content ranging from 12% to 50% depending on the binder used, for instance cement and lime, with the addition of fly ash and other additives (Colangelo et al., 2015; Geetha and Ramamurthy, 2010a; Tajra et al., 2018). Therefore, the prepared BCBLWAs have an even lower water content than other CBLAs. This is mainly due to the different microstructure and binder used. In cement-based pellets, the hydration products like C–S–H contain water. However, for carbonated steel slag, it contains a dense surface structure after calcite formation and also much compacted, that contains less water.

The water absorption of the prepared BCBLWAs is relatively low for SS100 to SS65MP35, reaching only 5.86%–18.83%. However, SS50MP50 has a much higher value of 41.06%. The interesting finding here is that with the 10 vol% MP in the BCBLWAs, the water absorption of prepared aggregate deceases from 5.86% to 5.09% compared to plain steel slag pellets. The reason may be that the formed calcite spreads on the surface of the MP and mitigates the water absorption of MP. However, for the last three mixes with more than 20 vol% MP, the water absorption increases very fast, and finally reaches 41.06%, which is higher than other CBLAs. For the cement-based binder aggregate with fly ash addition, the water absorption of CBLAs is from 10% to 30% as shown in Table 1 (Gomathi and Sivakumar, 2015; Güneyisi et al., 2015; Hwang and Tran, 2015; Thomas and Harilal, 2015). For the water content and absorption of this study, it is found that solely steel slag based aggregate has a much lower water content (1.14%) and water absorption (5.86%) than cement or lime based lightweight aggregate. High water adsorption of LWAs in concrete can be problematic, because the aggregate competes with the cement for water and thus increases the water demand of the whole concrete. On the other hand, using pre-saturated LWA can increase the time and cost of the preparation process and reduce the strength of the interface between aggregate and cement. Hence, carbonated steel slag incorporated with up to 35 vol% MP can be a good alternative.

Lightweight aggregate is defined in BS EN 13055 as any aggregate with a particle density of less than 2000 kg/m^3 or a dry loose bulk density of less than 1200 kg/m^3. Therefore, SS80MF20, SS65MF35, and SS50MP50 qualify as lightweight aggregates. SS100 and SS90MP10 do not meet the criterion but will be referred to with the same abbreviation BCBLWA for convenience. Overall, the density of BCBLWAs falls significantly with increased content of MP, the loose bulk density of SS80MP20, SS65MP35 and SS50MP50 are 1050 kg/m^3, 760 kg/m^3 and 550 kg/m^3, respectively.

The compressive strength of the individual BCBLWAs for each group is shown in Fig. 4. As can be seen in Fig. 4 (a), the maximum strength of BCBLWAs increases with the rising size of the aggregate. And this trend is more obvious for the groups containing less than 10% MP. This is due to the size effect on the stress of the aggregates and is in agreement with other researches (Tang et al., 2020b). It is interesting that SS90MP10 shows a steeper linear fit than other groups, indicating a higher strength or better carbonation effect and optimized MP content. MP first enhances and then decreases the individual pellet strength (IPS) of the aggregate with the rising MP content. It is obvious from the result that, up to a replacement level of 10%, IPS was enhanced continuously with an increase in the content of MP. Interestingly, the 10% MP dosage decreases the particle density and also improves the pellet strength. The decrease in density is attributed to the increase in MP fraction, which has a much lower density than steel slag. While the increase in IPS can be contributed by the high carbonation degree thanks to the MP providing more pathways for the CO_2 into the core of the aggregate, which can also be seen in the microstructure analysis. When the replacement ratio of MP is 20%–50%, the rising of MP content leads to a lower pellet strength compared to plain steel slag. This is because the MP itself has a very porous structure, and cannot provide sufficient strength to the aggregate, even function as a defect in the structure. Therefore, although more calcite could be formed in this high replacement ratio of MP, the mechanical performance was degraded due to the inherent low mechanical properties of MP. Hence, the best mechanical performance was achieved at a replacement ratio of 10% MP for BCBLWAs.

From Fig. 4 (b), it is obvious the calculated compressive strength is quite variable for each mix. Most of the aggregates show an evenly distributed strength regardless of their particle size. The strength development shows the sequence of SS90MP10 (4.18 MPa), SS100 (3.4 MPa), SS80MP20 (1.8 MPa), SS65MP35 (0.58 MPa) and SS50MP50 (0.12 MPa) as described in Table 7. However, the standard deviation is high. Therefore, bulk crushing resistance was used to further determine the strength of the BCBLWAs as shown in Table 7. As can be seen, the crushing resistance follows the same trend as the individual pellet strength. With the addition of 10% MP, the crushing resistance went up from 4.0 MPa to 4.8 MPa, while with increasing MP content the crushing resistance decreases to lower value, and the worst performance is shown by sample SS50MP50. This indicates a proper amount of MP can contribute to higher strength of BCBLWA, while excessive dosage of MP can lower the strength of BCBLWAs. Compared with other cold-bonded

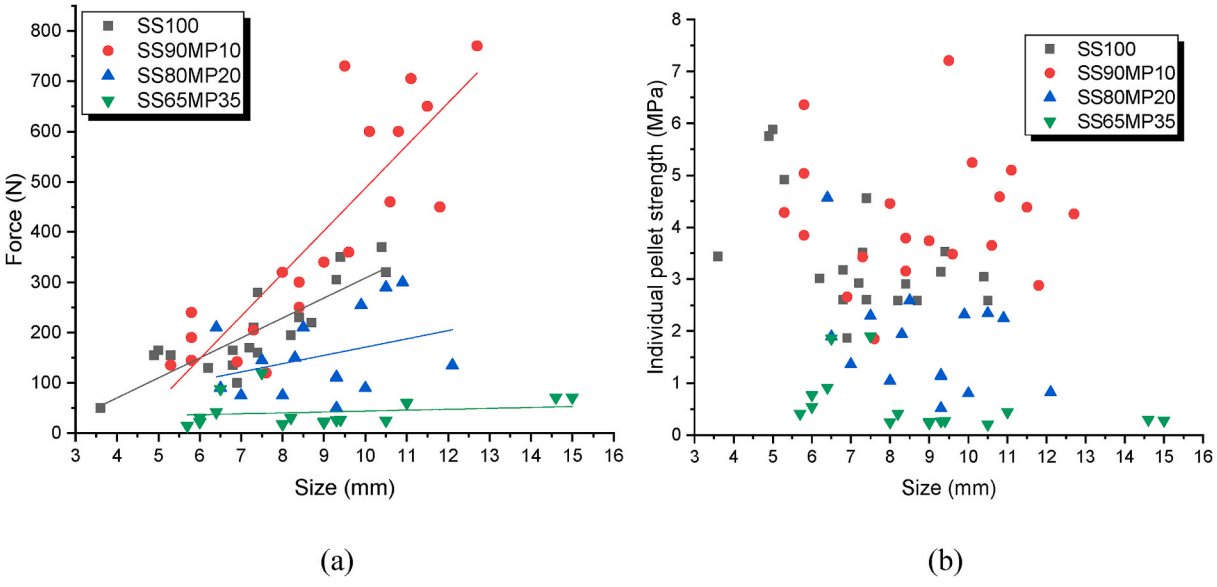

Fig. 4. Individual pellet stress (a) and strength (b) of different groups of BCBLWAs.

Table 7
Individual pellet strength and bulk crushing resistance of BCBLWAs.

Groups	SS100	SS90MP10	SS80MP20	SS65MP35	SS50MP50
Individual pellet strength (MPa)	3.4 ± 1.2	4.2 ± 1.53	1.8 ± 1.04	0.58 ± 0.29	0.12 ± 0.003
Bulk crushing resistance (MPa)	4.0 ± 0.3	4.8 ± 0.4	2.0 ± 0.2	0.99 ± 0.1	0.32 ± 0.06

lightweight aggregates, the strength of the prepared BCBLWAs is similar (Chi et al., 2003; Hwang and Tran, 2015; Kockal and Ozturan, 2011; Thomas and Harilal, 2015). Therefore, the strength mainly provided by the formation of calcite in the aggregate can offer similar strength to cement or lime based lightweight aggregate.

3.2. Reaction products and microstructure of BCBLWAs

3.2.1. XRD analysis

The X-ray diffraction pattern of the BCBLWAs with different amounts of miscanthus powder are shown in Fig. 5. The SS100 sample shows a very similar pattern as the raw steel slag shown in Fig. 2. The carbonation of the steel slag aggregate is very slow during the 3 days CO_2 curing. The main phases are wüstite, larnite and brownmillerite. Small amounts of magnetite are also present. The tiny peak emerging at 34.4° is the typical peak of calcite. However, the peak intensity of calcite is relatively low compared to other mixes with MP, showing that the SS100 aggregate is only partially carbonated and that the strength mainly comes from the compactness of the finely grounded steel slag.

After the addition of miscanthus powders, the XRD pattern changed and the calcite intensity increased with the increasing amount of MP. This trend is more obvious when 20% of MP was added. It can be seen from the peak at 34.4° that the calcite concentration increased significantly for the last three groups, which is in agreement with the TGA analysis in Section 3.2.2. And the peak of larnite and brownmillerite decreased and even hardly observed for group SS50MP50. This may due to the dilution effect because there is still some MP in the sample regardless of the pre-treatment. However, it still can be inferred that the carbonation could transform the minerals larnite C_2S and partially brownmillerite C_4AF into calcite. The XRDs show that small amount of

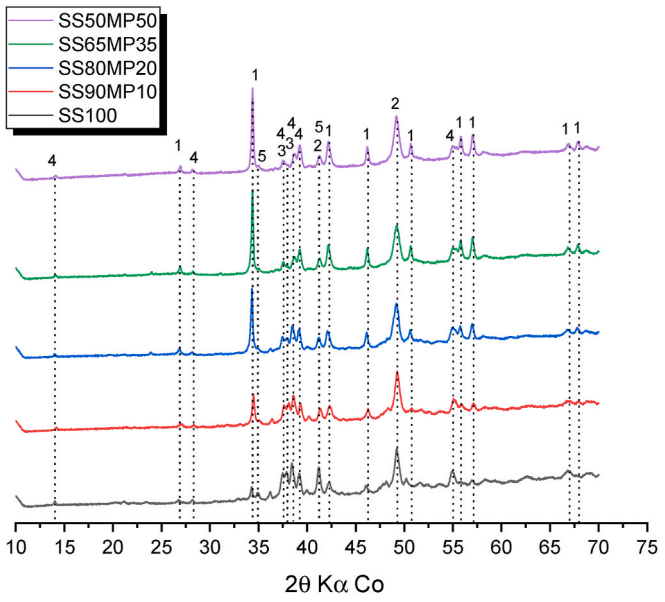

Fig. 5. XRD of the different kinds of BCBLWAs: 1- calcite 2- wüstite 3- larnite 4- brownmillerite 5- magnetite.

unreacted C_2S is still present so the carbonation could continue with longer CO_2 curing. The intensity of the wüstite (FeO) and magnetite (Fe_3O_4) peaks (49.1° and 35.1°) remains unchanged. Meanwhile, the silica that formed during carbonation is not visible in the XRD pattern, because it is amorphous.

3.2.2. TGA

The thermal gravimetry analysis of the produced BCBLWAs are presented in Fig. 6. There exist a few stages during the decomposition of the BCBLWAs. At the first stage, ranging from 40 to 105 °C, the loss of physical bonded water in the aggregates occurs. The second stage is the decomposition of miscanthus powder, ranging from 220 to 380 °C, due to the loss of organic component like cellulose and lignin (Nada and Hassan, 2000). The third stage is the decomposition of calcite, ranging from 650 to 800 °C, where the calcite formed in the aggregate during CO_2 curing decomposes to CaO and CO_2. It seems there is a fourth stage up until 1000 °C, this result may be due to the decomposition of lignin in the BCBLWAs, which needs further investigation (Waters et al., 2017).

As can be seen in Fig. 6, the BCBLWA produced with 100% steel slag shows the least amount of calcite present, reaching only 7.1 wt% in the artificial aggregates. While the 50SS50MP sample shows the largest calcite concentration among all the groups, reaching 27.7%. The calcite concentration of SS90MP10, SS80MP20 and SS65MP35 reached 7.6%, 16.4% and 24.5%, respectively, forming a clear trend.

Moreover, the CO_2 uptake of the BCBLWA aggregates is shown in Table 8. It is obvious the CO_2 uptake increases significantly with the rising MP content in the aggregate. The reference SS100 only adsorbs 4.17 wt%/g $_{(pellet)}$ CO_2, while for SS50MP50, this value increase to 16.43%/g. This can be interpreted as follows. Firstly, the CO_2 uptake in the aggregate is determined by the humidity, temperature and pore structure. More MP in the aggregate increases the porosity, thus providing more paths for CO_2 into the aggregate. Secondly, the water retained by the MP can provide more humidity than plain steel slag aggregate, creating a necessary water film on the slag surface accelerating carbonation (Supplementary Information Fig. S1). The phenolphthalein showed no colour after spraying onto the surface of a fractured SS65MP35 aggregate, further indicating the complete formation of calcite and consumption of $Ca(OH)_2$. In the SS100 sample the phenolphthalein still showed a red colour inside the aggregate. Therefore, it is confirmed that MP contributes to faster carbonation of steel slag in the aggregate and a higher CO_2 uptake of the artificial aggregates.

3.2.3. Nitrogen physisorption analysis

The nitrogen sorption isotherm and the pore size distribution of the prepared BCBLWAs are shown in Fig. 7. The reference SS100 sample and all other samples with miscanthus powder present the same type of physisorption isotherm. According to IUPAC definition, the isotherm is a type IV isotherm, meaning the aggregates have a mesoporous structure. The SS100 sample adsorbed a very low nitrogen quantity, while SS65MP35 shows a much higher amount of nitrogen absorbed. Consequently, the specific surface area of SS100 and SS65MP35 are 4.25 m^2/g and 20.64 m^2/g, respectively. This difference in surface area and absorbed nitrogen is due to the different microstructure of steel slag before and after carbonation. Firstly, the steel slag itself has very low intra-particle porosity hence the surface area is low. Also, the reference plain steel slag-based aggregate is so compacted that the carbonation effect on steel slag is very limited, leading to less carbonation products. Therefore, the surface area of SS100 is only slightly increased compared to uncarbonated steel slag (~2.0 m^2/g). While the addition of miscanthus powders contributes a route for CO_2 and moisture to get into the core of the aggregate and majority of the steel slag was carbonated. The carbonation of steel slag accelerates the formation of amorphous silica and calcite due to the reaction with C_2S in steel slag. The fact is the amorphous silica formed during carbonation shows a much higher surface area, normally from 50 m^2/g to 200 m^2/g according to literature (G. Liu et al., 2020). The calcite formed is also in the form of very fine

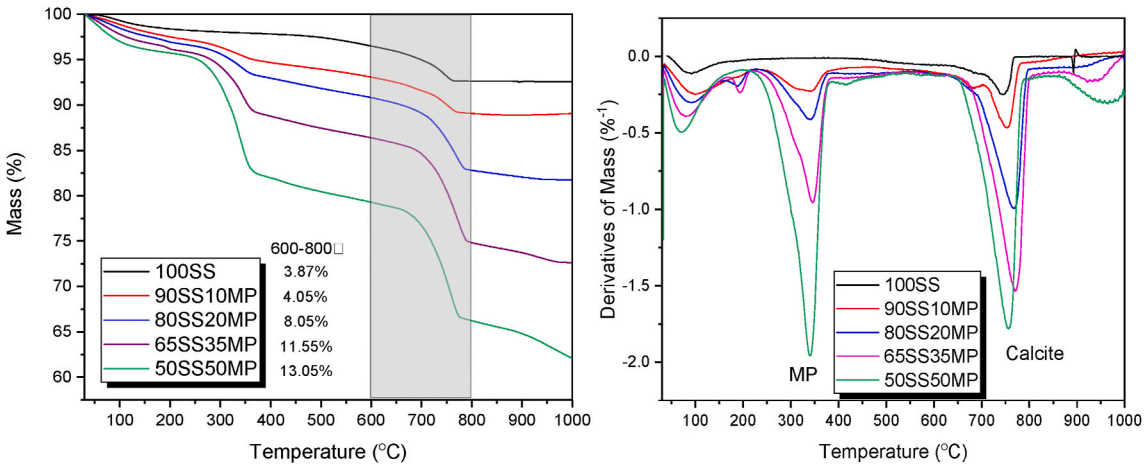

Fig. 6. Thermal gravimetric analysis of the synthesized BCBLWAs.

Table 8
CO_2 uptake capacity of each BCBLWA mix based on TG.

Group	SS100	SS90MP10	SS80MP20	SS65MP35	SS50MP50
CO_2 uptake (wt %/g pellets)	4.17	4.37	9.26	14.13	16.43

particles, which can also increase the specific surface area. Therefore, this is another indirect evidence that mesoporous silica with high surface area formed after carbonation. Also, this result is in agreement with the XRD and TGA analysis.

3.2.4. SEM

SEM pictures of fracture surface of BCBLWAs are presented in Fig. 8. As can be seen from Fig. 8 (a), the reference SS100 (plain carbonated steel slag aggregates) shows the morphology of discrete steel slag particles. The bonding between each particle is weak compared to other aggregates. The strength of the SS100 is mainly contributed by the compactness of steel slag and the thin carbonated outer surface of the aggregate. The inner structure is barely carbonated because the CO_2 cannot penetrate deeper into the inner structure.

However, with the addition of miscanthus powder, it is obvious that the bonding between steel slag particles is greatly enhanced by the formation of more calcite and amorphous silica. The phenomena are even more obvious when the MP content reaches a volume of 35%. As can be seen from Fig. 8 (d), more small and bright particles with a size below 10 μm are observed on the surface of MP, which indicates the formation of carbonation products from steel slag. Much more carbonation products are formed with a high surface area, resulting from a higher N_2 absorption than the pure SS100 sample.

It can be observed from Fig. S2 (overall view lower resolution) that much finer carbonation products are formed around the miscanthus powder than the area that far from MP. In Fig. 8 (c) and **(d)**, large amounts of finer carbonation products are formed inside the aggregates than the steel slag shown in Fig. 8 (a) and **(b)**, which is another evidence indicate the role of MP as the carbonation accelerator in BCBLWAs.

Therefore, it can be inferred from the SEM of BCBLWAs that with the incorporation of miscanthus powders, the porous structure of the MP provides the routes for CO_2 penetration, as a consequence, increasing the carbonation degree of steel slag inside the aggregate and also improving the bonding between particles by forming smaller size carbonation products that are below 10 μm in size.

3.2.5. Mechanism of carbonation reaction

The purpose of using MP in carbonated steel slag is to decrease the particle density and induce the carbonation reaction in the inner structure of BCBLWAs. As illustrated in Fig. 9 (a), the surface of the aggregate SS100 is carbonated after 3 days, forming a dense shell structure composed of calcite. The main CO_2 reactive component in converter steel slag is C_2S. C_2S can react with carbon dioxide and water to form calcite and silica gel as discussed above. The density of calcite (2.71 g/cm^3) and silica gel (2.65 g/cm^3) are smaller than C_2S (3.28 g/cm^3), thus the total volume of carbonation products will increase and fill

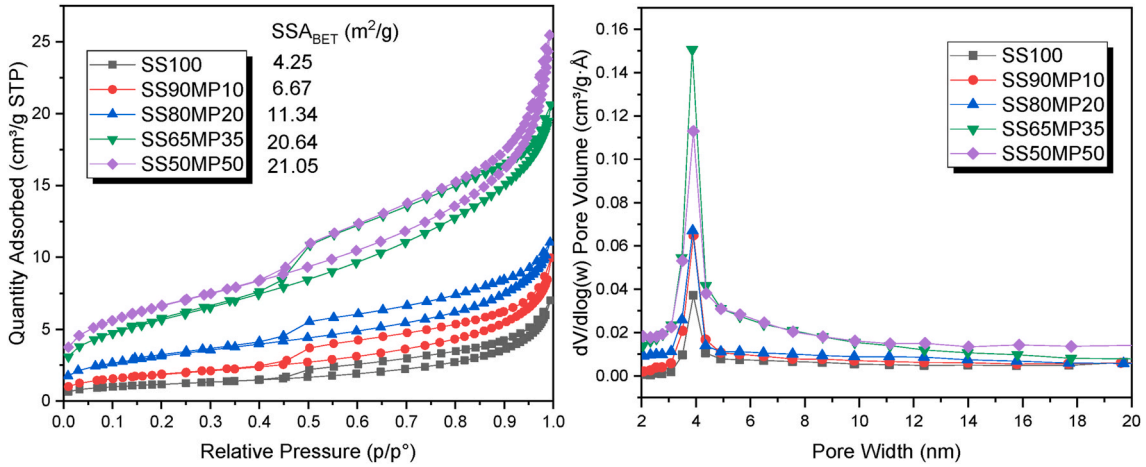

Fig. 7. Nitrogen isotherm and pore size distribution of different BCBLWAs.

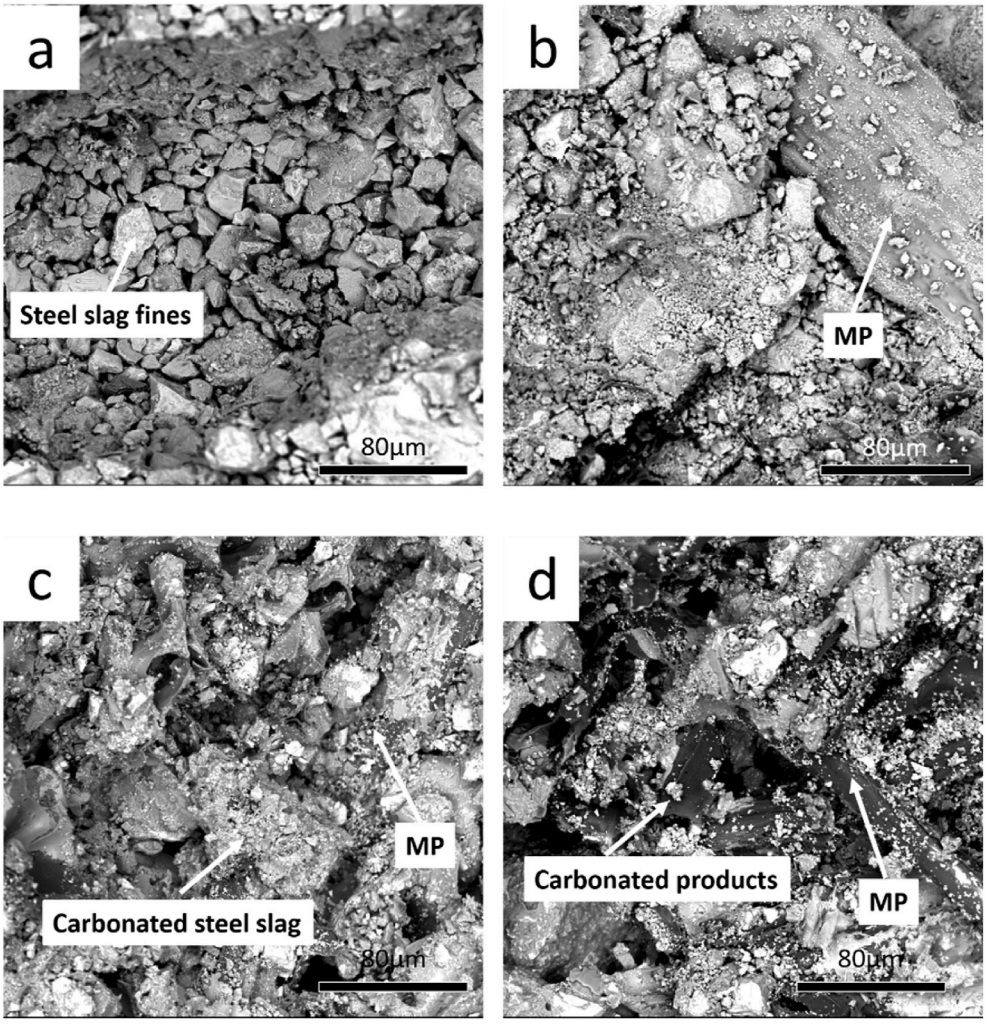

Fig. 8. SEM of BCBLWAs from different groups: (a) SS100 (b) SS90MP10 (c) SS80MP20 (d) SS65MP35.

in the inter-particle pores of steel slag, finally generate a much denser and ultralow porosity carbonation layer over the course of the 3-day CO_2 curing. However, the inner structure of the aggregate is barely carbonated, and are mainly compacted raw steel slag particles. Hence, the strength of the aggregate is primarily provided by the outer thinner shell structure of the aggregate. The dense calcite surface prevents the further CO_2 activation of the steel slag inside the aggregate, which means the transportation of CO_2 into the core of aggregate is limited.

Fig. 9 (b) shows the 10% MP addition in the aggregate can provide a 'shortcut' for the CO_2 to permeate deeper inside the compacted steel slag. The surface of the aggregate still first gets carbonated and form a medium dense shell structure. However, the MP change the packing of steel slag and allow more CO_2 pass through the intra-particle pores in the MP. Hence, the steel slag near MP can be carbonated faster and forms more calcite than steel slag located further. The water retained in the MP could also provide more intermedia for CO_2 activation, as the water film on the surface of steel slag particles accelerates the carbonation reaction (Baciocchi et al., 2015; Tu et al., 2015). This is because CO_2 has to first dissolve into the water to form CO_3^{2-} and then react with steel slag. Therefore, proper amount of MP benefits the mechanical performance of aggregate, regardless of the weak mechanical property of MP itself, which could be compromised.

The increase of MP dosage in the aggregate could induce more CO_2 reaction with steel slag, as illustrated in Fig. 9 (c). The MP provides more 'shortcuts' for CO_2 and moisture for transport into the cold-bonded particles, resulting in a complete carbonation of the aggregate, as evidenced by XRD result, showing most of the larnite are consumed by carbonation and forming calcite. This inference is also in accordance with the results of N_2 physisorption, as the surface area and gel pore volume of BCBLWA is the highest, indicating more carbonation products formed. However, due to the low mechanical performance of MP, the MP become the weak point or defect of the aggregate, thus decrease the strength. Therefore, excessive amount of MP degrades the strength of BCBLWAs. Hence, an optimal amount of MP is suggested in the production of BCBLWAs.

3.3. Lightweight concrete prepared with BCBLWAs

3.3.1. Density and strength of LWC-BCBLWAs

The density and strength of LWC-BCBLWAs with 50 vol% BCBLWAs at 7 and 28 days are presented in Fig. 10. Lightweight concrete is defined by BS EN 206–1 (EN206-1, 2005) as having an oven-dry density of not less than 800 kg/m^3 and not more than 2000 kg/m^3 by replacing dense natural aggregates either wholly or partially with lightweight aggregates. According to BS EN 206–1, all the LWC-BCBLWAs meet the criterial of lightweight concrete except for LWC-SS100 (2110 kg/m^3). The density of LWC-BCBLWAs ranges from 1852 to 1111 kg/m^3. The interesting finding here is the addition of SS90MP10 and SS80MP20 can not only lower the density of LWC-BCBLWAs, but also increase the compressive and flexural strength compared to concrete containing SS100. The reason is already explained in Section 3.2 and is owing to the optimal amount of MP allowing more calcite formation which

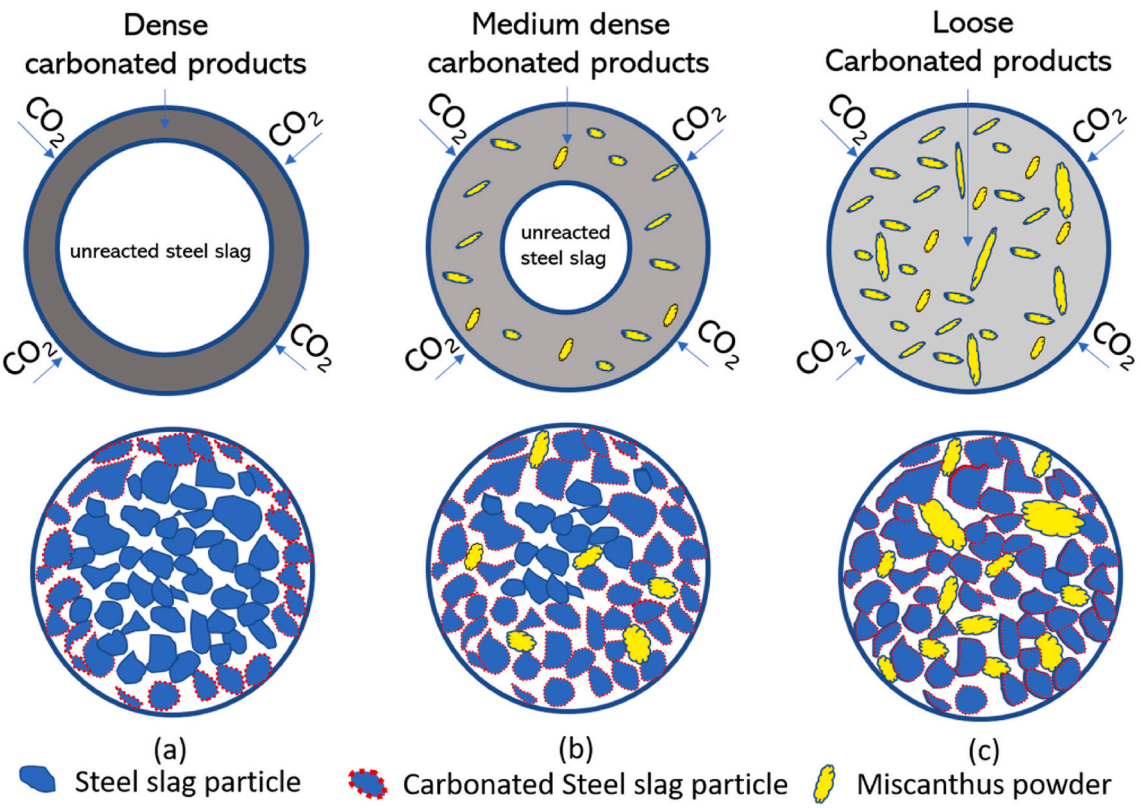

Fig. 9. Schematic illustration of inner structure of BCBLWAs: (a) SS100 (b) SS90MP10 (c) SS65MP35. The red dashed outline represents the carbonated steel slag, the blue shape outline represents the water film on the surface of miscanthus powder.

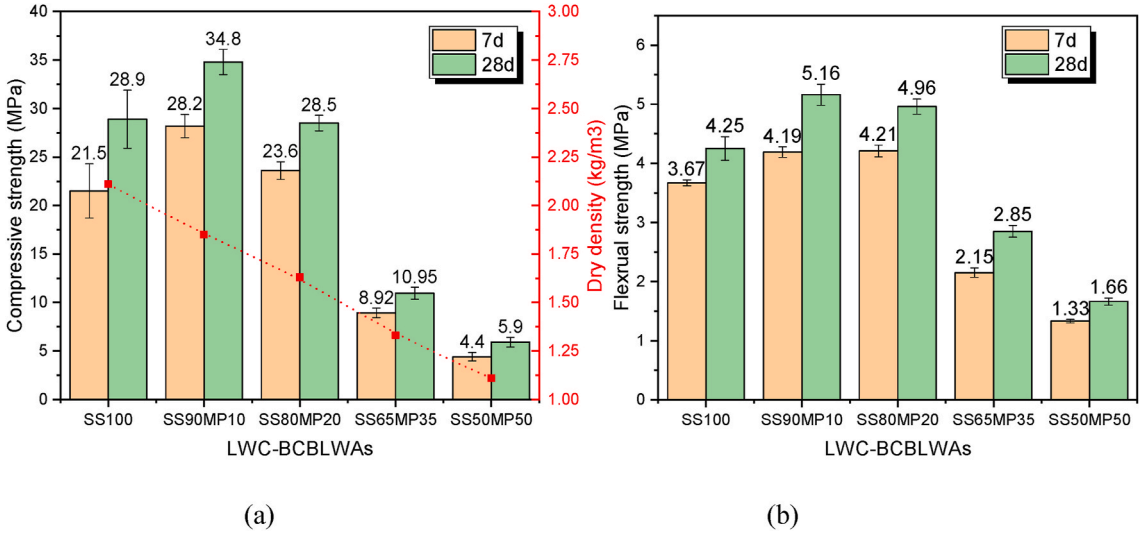

Fig. 10. Compressive (a) and flexural (b) strength of LWC-BCBLWAs at 7 and 28 days.

compensates for the low strength of the MP themselves.

For the groups with more MP incorporated in the aggregates, the strength of the lightweight concrete decreased significantly, and the dry density also reduced. This is expected if much lighter artificial aggregates are mixed in a cement matrix. For the LWC-SS50MP50, the compressive strength and flexural strength was 5.9 MPa and 1.66 MPa, respectively, while the dry density decreased to only 1111 kg/m^3. The sequence of strength is as follows: LWC-SS90MP10, LWC-SS80MP20, LWC-SS100, LWC-SS655MP35 and LWC-SS50MP50. According to literatures (Yu et al, 2013, 2015), a linear relationship exists between strength and density. However, in this study, the lower density of lightweight concrete not always indicates lower strength. Therefore, it is evidenced that 10% and 20% of MP in the BCBLWAs can increase the strength of the aggregate and consequently increase the strength of the lightweight concrete.

The facture surface after the flexural strength test is shown in Fig. 11. It is observed that all the BCBLWAs in the cement matrix are split due to the compression, much like the split of normal quartz aggregates. This is because of the strong interfacial bonding between BCBLWAs and hardened cement paste. Hence, the route of breaking was through BCBLWAs

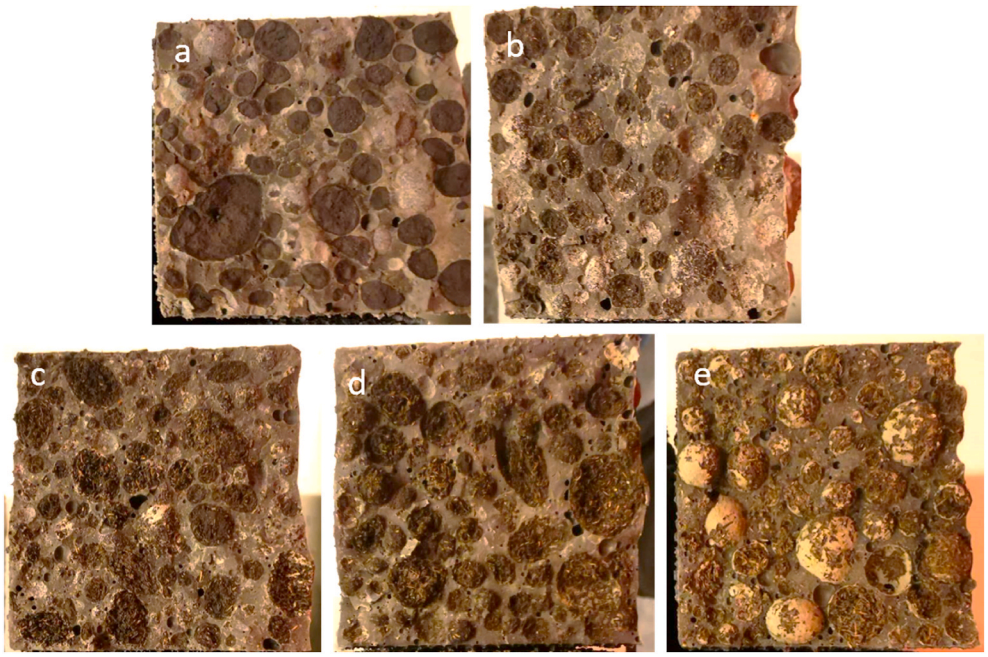

Fig. 11. Fracture surface of (a) LWC-SS100 (b) LWC-SS90MP10 (c) LWC-SS80MP20 (d) LWC-SS65MP35 (e) LWC-SS50MP50.

rather than through the interfacial transition zone (ITZ). Another reason is that the mechanical strength of BCBLWAs is much lower than that of hardened cement paste. Therefore, the strength of LWC-BCBLWAs is mainly dependent on the mechanical properties of BCBLWAs. However, it can be observed that the bonding between the cement paste and BCBLWAs is relatively weak for sample LWC-SS50MP50. It is possible that these aggregates take up a lot of water from the cement and then release it later, which creates a very porous low strength ITZ around the BCBLWAs, which is indicated by the spalling of aggregate from the hardened cement paste. Moreover, it is possible that the polysaccharides leached from miscanthus powder also negatively affect the strength development of ITZ and thus result in the interfacial zone as shown in Fig. 11 (e).

3.3.2. *Thermal conductivity of the LWC-BCBLWAs*

The thermal conductivity of plain SS100 lightweight concrete is 0.674 W/(m·K). While the thermal conductivity of other BCBLWAs is much lower as can be seen from Table 9. The SS90MP10, SS80MP20, SS65MP35 and SS50MP50 possess thermal conductivities of 0.545, 0.439, 0.369 and 0.255 W/(m·K), respectively. The higher MP concentration in the aggregates means more air voids are presented in the bio-lightweight aggregates. In the LWC-BCBLWAs, the thermal conductivity of the cement paste matrix is similar as the w/b ratio is consistent. While the influential factors are the different groups of BCBLWAs, which is supposed to have lower thermal conductivity with higher amount of MP. The plain cement paste (w/b = 0.5) and miscanthus powder have very different thermal conductivity, achieving 1.2 W/(m·K) and 0.1 W/(m·K), respectively. Therefore, as the replacement ratio of BCBLWAs kept as 50 vol% in the lightweight concrete, the thermal conductivity depends mainly on the types of bio-aggregates used. Thus, by applying miscanthus powder in the aggregate, it is highly possible to lower the thermal conductivity and consequently increase the overall thermal insulation of LWC-BCBLWAs. Other lightweight concrete with cold-bonded lightweight aggregate shows similar or higher thermal conductivity. Frankovic et al. (Frankovič et al., 2017) have found that cold-bonded aggregate concrete (CBAC) made with 100% CBLAs has a dry density of 1490 kg/m^3 and a thermal conductivity of 0.73 W/(m·K). Tajra et al. have also reported that the use of core-shell CBA allows the production of CBAC with a thermal conductivity of 0.64 W/(m·K) (Tajra et al., 2019).

The thermal conductivity versus the density of different kinds of lightweight concrete is shown in Fig. 12. The LWC-BCBLWAs have a slightly better compressive strength than other conventional lightweight concrete, for instance, pumice concrete and foam concrete (Schauerte and Trettin, 2012; Topçu and Uygunoğlu, 2010; Yu et al., 2015). The slope of the linear correlation between strength and thermal conductivity is significantly higher than for other LWCs. Therefore, the prepared LWC-BCBLWAs could obtain a good performance regarding thermal insulation and while still possessing sufficient strength at the same time. However, there is still potential to further lower the thermal conductivity of LWC-BCBLWAs, since the cement matrix used in this study is pure cement paste with w/b of 0.5. If the cement matrix can be further optimized by using an air-entraining agent and a hollow fly ash (Ferreira et al., 2016), the thermal conductivity could be lowered even further.

3.3.3. *The influence of BCBLWAs on the hydration of LWC-BCBLWA*

The effect of BCBLWAs on the hydration of Portland cement is interpreted using the calorimeter test. The hydration heat of three different groups of LWC-BCBLWAs is shown in Fig. 13. The hydration peak of the SS100 sample is the highest among all the groups, reaching the maximum heat release at 11 h. The SS100 sample shows almost the same time to reach the hydration peak as plain cement paste (10 h), according to literature (Chen et al., 2017), indicating carbonated steel slag itself has no retardation effect on cement paste. With rising content of MP in BCBLWAs, the time to reach hydration peak maximum

Table 9
Thermal conductivity of the developed LWC-BCBLWAs.

Groups	LWC-SS100	LWC-SS90MP10	LWC-SS80MP20	LWC-SS65MP35	LWC-SS50MP50
Thermal conductivity (W/(m·K))	0.674 ± 0.003	0.545 ± 0.002	0.439 ± 0.002	0.369 ± 0.004	0.255 ± 0.003

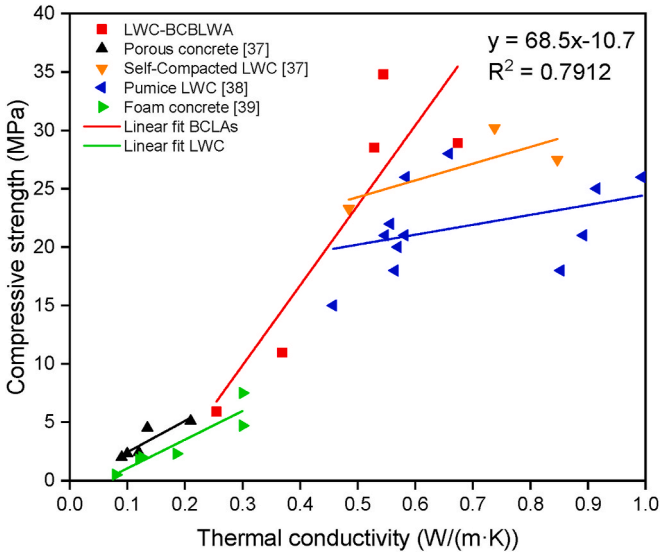

Fig. 12. Thermal conductivity versus compressive strength of different kinds of LWC.

increases which could be due to released polysaccharide by miscanthus. The SS80MP20 samples shows the hydration peak at 12 h. Meanwhile, SS65MP35 takes 12.5 h to reach the peak. MP by itself has a severe retardation effect on the cement hydration. If Miscanthus powder is added directly into the cement paste, the hydration peak maxima occurs only after 20 h (Chen et al., 2017). Hence, the delay of cement hydration is greatly mitigated by incorporating natural fibers into BCBLWAs. Therefore, the MP incorporated in steel slag-based binder shows less influence on the cement hydration. The steel slag fines surround the MP can contribute to the delay of the polysaccharide release from MP, resulting in less negative effect on the cement paste. Furthermore, the miscanthus is granulated which significantly reduces the surface area and amount of miscanthus that can leach polysaccharide. It is partially covered by carbonated slag and the miscanthus in the middle of the aggregate is probably not leach directly to the outer surface of the BCBLWAs. Therefore, it is a promising method to mitigate the retardation effect of miscanthus powders on the hydration of cement. Another reason should be the formation of amorphous silica, which can accelerate the hydration of cement and compensate the delay of cement hydration by polysaccharides. Overall, the cement hydration is only slightly delayed. The cumulative heat release also follows the same trend as the normalized heat release as shown in Fig. 13 (b).

3.4. CO_2 emission of lightweight concrete with BCBLWAs

One of the significant motivations of using carbonated steel slag and miscanthus is the high CO_2 uptake of BCBLWA aggregates and the low CO_2 emission of prepared lightweight concrete. The quantified CO_2 emissions of BCBLWAs and LWC-BCBLWAs are shown in Table 10 and Table 11. The CO_2 emission of finely grounded steel slag and miscanthus using disc mill are included, which is inferred as 0.1 kg CO_2/kg steel slag or miscanthus (G. Liu et al., 2020). The milling of steel slag and miscanthus increases CO_2 emission, however, the CO_2 uptake of milled steel slag can compensate for this, leading to a negative CO_2 emission in total. For miscanthus itself, thanks to the CO_2 sequestration during growth, the carbon dioxide equivalent mitigation potential is 117%/gram (Felten et al., 2013). Therefore, for the aggregates containing higher amounts of MP, the total CO_2 emission is much lower. As observed in Table 10, for 1 m^3 BCBLWAs, the increasing dosage of MP in the aggregate decreases the total CO_2 emission significantly. Firstly, the CO_2 uptake capacity of the BCBLWAs is much higher than plain steel slag, as calculated from TGA in Table 8. Secondly, the MP itself have a high CO_2 absorption capacity than steel slag. Therefore, the artificial aggregate containing 20 vol% MP starts to obtain a negative CO_2 emission of −92.8 kg/m^3.

Table 11 shows the lightweight concrete incorporated with BCBLWAs also features low CO_2 emission than plain steel slag aggregate concrete. For LWC-SS100, the CO_2 emission is 574.2 kg/m^3, due to the cement and finely grounded steel slag produce large amount of CO_2, while the CO_2 uptake of plain SS100 aggregate is the lowest among the

Table 10
CO_2 emission of BCBLWAs (1 m^3).

CO_2 emission	SS100	SS90MP10	SS80MP20	SS65MP35	SS50MP50
Steel slag (milling)	163.0	124.7	96.4	63.7	40.5
Miscanthus (milling)	0	5.3	8.6	12.3	14.5
CO_2 uptake (BCBLWAs)	−67.9	−56.8	−97.2	−107.3	−90.3
CO_2 absorption (Miscanthus)	0	−62.01	−100.6	−143.9	−169.6
CO_2 curing	0.025	0.025	0.025	0.025	0.025
Total CO_2 emission for BCBLWAs	95.1	11.2	−92.8	−175.2	−204.9

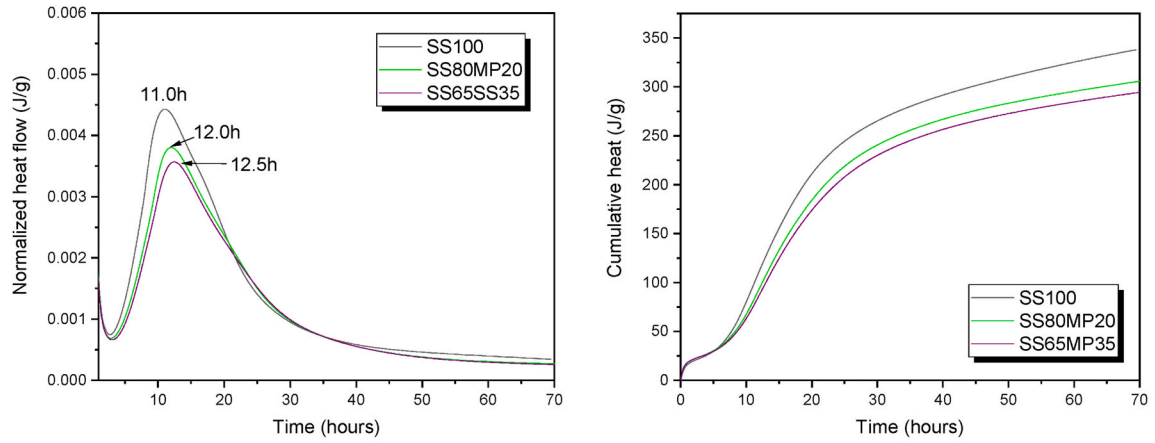

Fig. 13. The calorimeter test of BCBLWAs incorporated cement paste with an aggregate volume ratio of 0.5: (a) Normalized heat release (b) Cumulative heat.

Table 11
CO_2 emission of prepared lightweight concrete with 50 vol% BCBLWAs for 1 m^3.

CO_2 emission	LWC-SS100	LWC-SS90MP10	LWC-SS80MP20	LWC-SS65MP35	LWC-SS50MP50
Cement	492.5	492.5	492.5	492.5	492.5
Steel slag (milling)	140.5	100.7	82.6	62.8	36.7
Miscanthus(milling)	0	4.3	7.4	12.5	13.3
Water	0.04	0.04	0.04	0.04	0.04
CO_2 uptake (BCBLWAs)	−58.8	−46.2	−83.3	−106.0	−82.15
CO_2 absorption (Miscanthus)	0	−50.3	−86.6	−142.2	−155
CO_2 for curing	0.025	0.025	0.025	0.025	0.025
Total CO_2 emission of LWC-BCBLWAs	574.2	501.0	412.6	319.6	305.0

five groups. With the utilization of BCBLWAs in the lightweight concrete, the CO_2 uptake capacity of bio-aggregate rises significantly as presented in Table 10, thus compensates the high CO_2 emission of cement and the usage of disc mill. The lowest CO2 emission reaches 305.0 kg/m^3 for LWC-SS50MP50. Therefore, the utilization of BCBLWAs in LWC significantly reduce the embedded CO_2 footprint and thus more sustainable. These results demonstrate that the optimal combination of carbonated steel slag and miscanthus powder can result in a much lower CO_2 emission than normal lightweight concrete.

4. Conclusions

The cement-free bio-based cold-bonded lightweight aggregate (BCBLWAs) using steel slag and miscanthus powders via CO_2 curing was developed and investigated. The prepared BCBLWAs features a low density, low water absorption and high CO_2 uptake capacity. Lightweight concrete utilizing as-prepared BCBLWAs shows low density, relatively high strength and superior thermal insulation properties. The following conclusions can be drawn based on the study:

1. The miscanthus powders can provide additional routes for CO_2 transportation in prepared aggregate, thus contributing to a more rapid carbonation process of steel slag particles. However, high content of miscanthus powder can result in a porous structure of BCBLWAs, as well as low strength. Sample with 10 vol% miscanthus powder shows the best strength performance, which increases by 20% compared to plain carbonated steel slag.
2. The carbonation products of BCBLWAs are mainly calcite and amorphous silica. The calcite acts as a binding agent and increases the mechanical properties of BCBLWAs. Contrary to cement hydration, carbonation was not affected by the presence of polysaccharides leaching from the miscanthus powder, which makes it an effective strategy for producing cold bonded aggregates containing natural fibers. The pelletization also covers the miscanthus powder in carbonation products and reduces their water adsorption, which makes it possible to use them in OPC based concrete.
3. Concrete incorporating BCBLWAs meets the standard of lightweight concrete and the strength is relatively high for concrete using BCBLWAs with 10 vol% miscanthus powder, reaching a strength of 34.8 MPa at 28 d. The bonding between BCBLWAs and cement paste is negatively impacted if very high amounts of miscanthus powder are used in the aggregate as the fracture happens at the surface of BCBLWAs rather than at the interface. This also results in lower mechanical strength of the concrete. More work is needed to investigate this and find a method to enhance the interface when high amounts of miscanthus are incorporated into BCBLWAs.
4. The thermal conductivity of LWC-BCBLWAs deceased to 0.255 W/(m·K) when 50% SS50MP50 used in lightweight concrete. Furthermore, the density dropped to 1100 kg/m^3. The thermal insulation property of LWC-BCBLWAs are projected to have a better performance than other non-plant based lightweight concrete.

This study shows that the use of carbonation makes it possible to avoid the problem of cement and bio-fibers incompatibility without additional treatment of the bio-fibers. This method could be applied to other biomaterials that leach even more polysaccharide than miscanthus, for instance, coconut fibers or hemp fibers as well saw dust. More research about the performance and durability of BCBLWAs under different conditions will be carried out in the future, for instance, hygrothermal properties in high humidity condition and fire resistance performance.

Declaration of competing interest

The authors declare that they have no known competing financial interests or personal relationships that could have appeared to influence the work reported in this paper.

Acknowledgement

This research is supported by China Scholarship Council (CSC) Fund (Grant No. 201706950053), Xi'an Jiaotong University and Eindhoven University of Technology. Vibers (the Netherlands), Tata steel (the Netherlands), ENCI (the Netherlands) are thanked for providing materials.

Appendix A. Supplementary data

Supplementary data to this article can be found online at https://doi.org/10.1016/j.jclepro.2021.129105.

References

Baciocchi, R., Costa, G., Polettini, A., Pomi, R., 2015. Effects of thin-film accelerated carbonation on steel slag leaching. J. Hazard Mater. 286, 369–378. https://doi.org/10.1016/j.jhazmat.2014.12.059.

Barra, M., Aponte, D., Vazquez, E., Mendez, B., Miro, R., Valls, S., 2016. Experimental study of the effect of the thermal conductivity of EAF slag aggregates used in asphaltic concrete of wearing courses on the durability of road pavements. Sustain. Constr. Mater. Technol. 2016-Augus. https://doi.org/10.18552/2016/scmt4d140.

Baykal, G., Döven, A.G., 2000. Utilization of fly ash by pelletization process; theory, application areas and research results. Resour. Conserv. Recycl. 30, 59–77. https://doi.org/10.1016/S0921-3449(00)00042-2.

Belhadj, E., Diliberto, C., Lecomte, A., 2012. Characterization and activation of basic oxygen furnace slag. Cement Concr. Compos. 34, 34–40. https://doi.org/10.1016/j.cemconcomp.2011.08.012.

Bheel, N., Sohu, S., Awoyera, P., Kumar, A., Abbasi, S.A., Olalusi, O.B., 2021. Effect of wheat straw ash on fresh and hardened concrete reinforced with jute fiber. Adv. Civ. Eng. 2021 https://doi.org/10.1155/2021/6659125.

Bui, L.A.T., Hwang, C.L., Chen, C.T., Lin, K.L., Hsieh, M.Y., 2012. Manufacture and performance of cold bonded lightweight aggregate using alkaline activators for high performance concrete. Construct. Build. Mater. 35, 1056–1062. https://doi.org/10.1016/j.conbuildmat.2012.04.032.

Chandra, S., Berntsson, L., 2002. Introduction. In: Chandra, S., Berntsson, L.B.T.-L.A.C. (Eds.), Lightweight Aggregate Concrete. William Andrew Publishing, Norwich, NY, pp. 1–3. https://doi.org/10.1016/B978-081551486-2.50003-1.

Chen, Y., Yu, Q.L., Brouwers, H.J.H.H., 2017. Acoustic performance and microstructural analysis of bio-based lightweight concrete containing miscanthus. Construct. Build. Mater. 157, 839–851. https://doi.org/10.1016/j.conbuildmat.2017.09.161.

Chen, Y.X., Wu, F., Yu, Q., Brouwers, H.J.H.H., 2020. Bio-based ultra-lightweight concrete applying miscanthus fibers: acoustic absorption and thermal insulation. Cement Concr. Compos. 114, 103829 https://doi.org/10.1016/j.cemconcomp.2020.103829.

Chi, J.M., Huang, R., Yang, C.C., Chang, J.J., 2003. Effect of aggregate properties on the strength and stiffness of lightweight concrete. Cement Concr. Compos. 25, 197–205. https://doi.org/10.1016/S0958-9465(02)00020-3.

Colangelo, F., Messina, F., Cioffi, R., 2015. Recycling of MSWI fly ash by means of cementitious double step cold bonding pelletization: technological assessment for the production of lightweight artificial aggregates. J. Hazard Mater. 299, 181–191. https://doi.org/10.1016/j.jhazmat.2015.06.018.

Di Palma, L., Medici, F., Vilardi, G., 2015. Artificial aggregate from non metallic automotive shredder residue. Chem. Eng. Trans. 43, 1723–1728. https://doi.org/10.3303/CET1543288.

Ducman, V., Mladenovic, A., 2002. Lightweight aggregate based on waste glass and its alkali – silica reactivity. Cement Concr. Res. 32, 223–226.

EN1097-3, 1998. Tests for Mechanical and Physical Properties of Aggregates-Part 3: Determination of Loose Bulk Density and Voids. Germany.

EN1097-6, 2005. Tests for Mechanical and Physical Properties of Aggregates – Part 6: Determination of Particle Density and Water Absorption. Germany.

EN13055-1, 2002. Lightweight Aggregates — Part 1: Lightweight Aggregates for Concrete, Mortar and Grout.

EN206-1, 2005. Concrete Part 1: Specification, Performance, Production and Conformity.

EUROFER, 2019. European Steel in Figures 2019 [WWW Document]. URL. https://www.eurofer.eu/publications/archive/european-steel-in-figures-2019/.

Fan, M., Ndikontar, M.K., Zhou, X., Ngamveng, J.N., 2012. Cement-bonded composites made from tropical woods: compatibility of wood and cement. Construct. Build. Mater. 36, 135–140. https://doi.org/10.1016/j.conbuildmat.2012.04.089.

Felten, D., Fröba, N., Fries, J., Emmerling, C., 2013. Energy balances and greenhouse gas-mitigation potentials of bioenergy cropping systems (Miscanthus, rapeseed, and maize) based on farming conditions in Western Germany. Renew. Energy 55, 160–174. https://doi.org/10.1016/j.renene.2012.12.004.

Ferreira, V.J., Sáez-De-Guinoa Vilaplana, A., García-Armingol, T., Aranda-Usón, A., Lausín-González, C., López-Sabirón, A.M., Ferreira, G., 2016. Evaluation of the steel slag incorporation as coarse aggregate for road construction: technical requirements and environmental impact assessment. J. Clean. Prod. 130, 175–186. https://doi.org/10.1016/j.jclepro.2015.08.094.

Franković, A., Bosiljkov, V.B., Ducman, V., 2017. Lightweight aggregates made from fly ash using the cold-bond process and their use in lightweight concrete. Mater. Tehnol. 51, 267–274. https://doi.org/10.17222/mit.2015.337.

Geetha, S., Ramamurthy, K., 2013. Properties of geopolymerised low-calcium bottom ash aggregate cured at ambient temperature. Cement Concr. Compos. 43, 20–30. https://doi.org/10.1016/j.cemconcomp.2013.06.007.

Geetha, S., Ramamurthy, K., 2010a. Environmental friendly technology of cold-bonded bottom ash aggregate manufacture through chemical activation. J. Clean. Prod. 18, 1563–1569. https://doi.org/10.1016/j.jclepro.2010.06.006.

Geetha, S., Ramamurthy, K., 2010b. Reuse potential of low-calcium bottom ash as aggregate through pelletization. Waste Manag. 30, 1528–1535. https://doi.org/10.1016/j.wasman.2010.03.027.

Gesoğlu, M., Güneyisi, E., Öz, H.Ö., 2012. Properties of lightweight aggregates produced with cold-bonding pelletization of fly ash and ground granulated blast furnace slag. Mater. Struct. Constr. 45, 1535–1546. https://doi.org/10.1617/s11527-012-9855-9.

Gomathi, P., Sivakumar, A., 2015. Accelerated curing effects on the mechanical performance of cold bonded and sintered fly ash aggregate concrete. Construct. Build. Mater. 77, 276–287. https://doi.org/10.1016/j.conbuildmat.2014.12.108.

Güneyisi, E., Gesołlu, M., Altan, I., Öz, H.Ö., 2015. Utilization of cold bonded fly ash lightweight fine aggregates as a partial substitution of natural fine aggregate in self-compacting mortars. Construct. Build. Mater. 74, 9–16. https://doi.org/10.1016/j.conbuildmat.2014.10.021.

Hwang, C.L., Tran, V.A., 2015. A study of the properties of foamed lightweight aggregate for self-consolidating concrete. Construct. Build. Mater. 87, 78–85. https://doi.org/10.1016/j.conbuildmat.2015.03.108.

Jiang, Y., Ling, T.C., Shi, M., 2020. Strength enhancement of artificial aggregate prepared with waste concrete powder and its impact on concrete properties. J. Clean. Prod. 257, 120515 https://doi.org/10.1016/j.jclepro.2020.120515.

Kockal, N.U., Ozturan, T., 2011. Durability of lightweight concretes with lightweight fly ash aggregates. Construct. Build. Mater. 25, 1430–1438. https://doi.org/10.1016/j.conbuildmat.2010.09.022.

Liu, G., Schollbach, K., van der Laan, S., Tang, P., Florea, M.V.A., Brouwers, H.J.H., 2020a. Recycling and utilization of high volume converter steel slag into CO2 activated mortars – the role of slag particle size. Resour. Conserv. Recycl. 160 https://doi.org/10.1016/j.resconrec.2020.104883.

Liu, Q., Song, Z., Han, H., Donkor, S., Jiang, L., Wang, W., Chu, H., 2020b. A novel green reinforcement corrosion inhibitor extracted from waste Platanus acerifolia leaves. Construct. Build. Mater. 260, 119695 https://doi.org/10.1016/j.conbuildmat.2020.119695.

Liu, Y., Song, Z., Wang, W., Jiang, L., Zhang, Y., Guo, M., Song, F., Xu, N., 2019. Effect of ginger extract as green inhibitor on chloride-induced corrosion of carbon steel in simulated concrete pore solutions. J. Clean. Prod. 214, 298–307. https://doi.org/10.1016/j.jclepro.2018.12.299.

Moll, L., Wever, C., Völkering, G., Pude, R., 2020. Increase of Miscanthus cultivation with new roles in materials production—a review. Agronomy 10, 8–11. https://doi.org/10.3390/agronomy10020308.

Nada, A.M.A., Hassan, M.L., 2000. Thermal behavior of cellulose and some cellulose derivatives. Polym. Degrad. Stabil. 67, 111–115. https://doi.org/10.1016/S0141-3910(99)00100-7.

Papadopoulos, A.P., Bar-Tal, A., Silber, A., Saha, U.K., Raviv, M., 2008. Inorganic and Synthetic Organic Components of Soilless Culture and Potting Mixes. In: Raviv, M., Lieth, J.H.B.T.-S.C. (Eds.). Elsevier, Amsterdam, pp. 505–543. https://doi.org/10.1016/B978-044452975-6.50014-9.

Pude, R., Treseler, C.H., Noga, G., 2004. Morphological, chemical and technical parameters of Miscanthus genotypes. J. Appl. Bot. Food Qual. 78, 58–63.

Ramamurthy, K., Harikrishnan, K.I., 2006. Influence of binders on properties of sintered fly ash aggregate. Cement Concr. Compos. 28, 33–38. https://doi.org/10.1016/j.cemconcomp.2005.06.005.

Reddy, K.R., Chetri, J.K., Kumar, G., Grubb, D.G., 2019. Effect of basic oxygen furnace slag type on carbon dioxide sequestration from landfill gas emissions. Waste Manag. 85, 425–436. https://doi.org/10.1016/j.wasman.2019.01.013.

Schauerte, M., Trettin, R., 2012. Neue Schaumbetone mit gesteigerten mechanischen ind physikalischen Eigenschaften. In: Proceedings of the 18th Ibausil, International Conference on Building Materials.

Tajra, F., Abd Elrahman, M., Lehmann, C., Stephan, D., 2019. Properties of lightweight concrete made with core-shell structured lightweight aggregate. Construct. Build. Mater. 205, 39–51. https://doi.org/10.1016/j.conbuildmat.2019.01.194.

Tajra, F., Elrahman, M.A., Chung, S.Y., Stephan, D., 2018. Performance assessment of core-shell structured lightweight aggregate produced by cold bonding pelletization process. Construct. Build. Mater. 179, 220–231. https://doi.org/10.1016/j.conbuildmat.2018.05.237.

Tang, P., Brouwers, H.J.H., 2018. The durability and environmental properties of self-compacting concrete incorporating cold bonded lightweight aggregates produced from combined industrial solid wastes. Construct. Build. Mater. 167, 271–285. https://doi.org/10.1016/j.conbuildmat.2018.02.035.

Tang, P., Brouwers, H.J.H., 2017. Integral recycling of municipal solid waste incineration (MSWI) bottom ash fines (0–2 mm) and industrial powder wastes by cold-bonding pelletization. Waste Manag. 62, 125–138. https://doi.org/10.1016/j.wasman.2017.02.028.

Tang, P., Florea, M.V.A., Brouwers, H.J.H., 2017. Employing cold bonded pelletization to produce lightweight aggregates from incineration fine bottom ash. J. Clean. Prod. 165, 1371–1384. https://doi.org/10.1016/j.jclepro.2017.07.234.

Tang, P., Xuan, D., Cheng, H.W., Poon, C.S., Tsang, D.C.W., 2020a. Use of CO2 curing to enhance the properties of cold bonded lightweight aggregates (CBLAs) produced with concrete slurry waste (CSW) and fine incineration bottom ash (IBA). J. Hazard Mater. 381 https://doi.org/10.1016/j.jhazmat.2019.120951.

Tang, P., Xuan, D., Li, J., Cheng, H.W., Poon, C.S., Tsang, D.C.W., 2020b. Investigation of cold bonded lightweight aggregates produced with incineration sewage sludge ash (ISSA) and cementitious waste. J. Clean. Prod. 251 https://doi.org/10.1016/j.jclepro.2019.119709.

Tang, P., Xuan, D., Poon, C.S., Tsang, D.C.W., 2019. Valorization of concrete slurry waste (CSW) and fine incineration bottom ash (IBA) into cold bonded lightweight aggregates (CBLAs): feasibility and influence of binder types. J. Hazard Mater. 368, 689–697. https://doi.org/10.1016/j.jhazmat.2019.01.112.

Thomas, J., Harilal, B., 2015. Properties of cold bonded quarry dust coarse aggregates and its use in concrete. Cement Concr. Compos. 62, 67–75. https://doi.org/10.1016/j.cemconcomp.2015.05.005.

Topçu, I.B., Uygunoğlu, T., 2010. Effect of aggregate type on properties of hardened self-consolidating lightweight concrete (SCLC). Construct. Build. Mater. 24, 1286–1295. https://doi.org/10.1016/j.conbuildmat.2009.12.007.

Tu, M., Zhao, H., Lei, Z., Wang, L., Chen, D., Yu, H., Qi, T., 2015. Aqueous carbonation of steel slag: a kinetics study. ISIJ Int. 55, 2509–2514. https://doi.org/10.2355/isijinternational.ISIJINT-2015-142.

C.I.C. Wang, G.C., 2016. 1 - Introduction. In: Wang, G.C.B.T.-T.U. of S. (Ed.). Woodhead Publishing, pp. 1–7. https://doi.org/10.1016/B978-0-08-100381-7.00001-X.

Wang, Q., Yan, P., 2010. Hydration properties of basic oxygen furnace steel slag. Construct. Build. Mater. 24, 1134–1140. https://doi.org/10.1016/j.conbuildmat.2009.12.028.

Waters, C.L., Janupala, R.R., Mallinson, R.G., Lobban, L.L., 2017. Staged thermal fractionation for segregation of lignin and cellulose pyrolysis products: an experimental study of residence time and temperature effects. J. Anal. Appl. Pyrolysis 126, 380–389. https://doi.org/10.1016/j.jaap.2017.05.008.

Yu, Q.L., Spiesz, P., Brouwers, H.J.H., 2015. Ultra-lightweight concrete: conceptual design and performance evaluation. Cement Concr. Compos. 61, 18–28. https://doi.org/10.1016/j.cemconcomp.2015.04.012.

Yu, Q.L., Spiesz, P., Brouwers, H.J.H., 2013. Development of cement-based lightweight composites - Part 1: mix design methodology and hardened properties. Cement Concr. Compos. 44, 17–29. https://doi.org/10.1016/j.cemconcomp.2013.03.030.